Cyaphide-alkynyl complexes: metal-ligand conjugation and the influence of remote substituents

Article (Accepted Version)

Dalton Transactions

Accepted Manuscript

This article can be cited before page numbers have been issued, to do this please use: S. K. Furfari, M. C. Leech, N. Trathen, M. C. Levis and I. R. Crossley, *Dalton Trans.*, 2019, DOI: 10.1039/C9DT01071H.

This is an Accepted Manuscript, which has been through the Royal Society of Chemistry peer review process and has been accepted for publication.

Accepted Manuscripts are published online shortly after acceptance, before technical editing, formatting and proof reading. Using this free service, authors can make their results available to the community, in citable form, before we publish the edited article. We will replace this Accepted Manuscript with the edited and formatted Advance Article as soon as it is available.

You can find more information about Accepted Manuscripts in the author guidelines.

Please note that technical editing may introduce minor changes to the text and/or graphics, which may alter content. The journal's standard Terms & Conditions and the ethical guidelines, outlined in our author and reviewer resource centre, still apply. In no event shall the Royal Society of Chemistry be held responsible for any errors or omissions in this Accepted Manuscript or any consequences arising from the use of any information it contains.

ROYAL SOCIETY OF CHEMISTRY

rsc.li/dalton

View Article Online
DOI: 10.1039/C9DT01071H

Dalton Transactions

ARTICLE

Cyaphide-alkynyl complexes: Metal-ligand conjugation and the influence of remote substituents†

Received 00th January 20xx,
Accepted 00th January 20xx

DOI: 10.1039/x0xx00000x

www.rsc.org/

Samantha K. Furfari, Matthew C. Leech, Nicola Trathen, Madeleine C. Levis and Ian R. Crossley*

A homologous series of novel *trans*-cyaphide-alkynyl complexes, *viz*. *trans*-[Ru(dppe)$_2$(C≡P)(C≡CC$_6$H$_4$R-*p*)] (R = Me, H, F, CO$_2$Me, NO$_2$) is prepared and comprehensively characterised, alongside their parent phosphaalkyne-complex cations *trans*-[Ru(dppe)$_2$(η^1-P≡CSiMe$_3$)(C≡CC$_6$H$_4$R-*p*)]$^+$. Structural data for *trans*-[Ru(dppe)$_2$(C≡P)(C≡CC$_6$H$_4$R-*p*)] (R = Me, F) and *trans*-[Ru(dppe)$_2$(η^1-P≡CSiMe$_3$)(C≡CC$_6$H$_4$R-*p*)]$^+$ (R = F, CO$_2$Me) are described, along with that for the previously reported *trans*-[Ru(dppe)$_2$(C≡P)(C≡CCO$_2$Me)]. NMR spectroscopic data indicate significant influence of the remote aromatic substituent over the properties of the cyaphide ligand, in line with the Hammett parameter (σ$_p$), suggesting appreciable 'communication' along the through-conjugate chain. Cyclic voltammety shows irreversible oxidative behaviour, at more anodic E_{pa} than in the respective alkynyl-chloride complexes, though apparently moderated by the remote substituent.

Introduction

Phosphaalkynes are among the best established and most studied classes of low-coordinate phosphacarbon.[1] Their chemistry epitomizes the phosphorus-carbon analogy[2] with a prevalence of alkyne-like behaviour, a corollary of the π-centred HOMO and heavily stabilised phosphorus lone-pair. Thus, extensive cycloaddition and oligomerisation chemistry is known,[3] and exploited *en-route* to organophosphorus architectures. In an organometallic context, metal-centred cyclization is common,[4] resulting from the preferential adoption of the η^2-P≡C-R coordination mode, albeit that nitrile-like η^1-P coordination can be induced within encumbered coordination spheres.[5] Indeed, steric encumbrance is widely invoked to achieve kinetic stability of the core 'P≡C' fragment, albeit that electronic factors are now recognised to be equally important,[6] as clearly illustrated by recent prevalent activity with the phosphaethynyloate ion '$^-$OC≡P'.[7]

Notwithstanding, the simplest phosphacarbon fragment, *viz.* the cyaphide ('$^-$C≡P') moiety, a direct analogue of terminal ethynyl ('$^-$C≡CH'), long remained elusive, the free anion being computed to be intrinsically unstable.[8] Only in 1992 was this ligand first described, with Angelici's *in situ* observation of *trans*-Pt(PEt$_3$)$_2$Cl(C≡P),[9] albeit only isolable by coordination of the reactive π-system within the structurally characterised [(Et$_3$P)$_2$PtCl(μ-η^1:η^2-C≡P)Pt(PEt$_3$)$_2$].[9,10] The unequivocal observation of a terminal cyaphide ligand was finally achieved in 2006, with Grützmacher's seminal report of *trans*-[RuH(dppe)$_2$(C≡P)] (**1**),[11] obtained by desilylative rearrangement of the parent *trans*-[RuH(dppe)$_2$(η^1-P≡CSiPh$_3$)]$^+$ (**2**$^+$). The stability of **1** was attributed to the steric protection afforded by the 'M(dppe)$_2$' scaffold, which has also featured heavily in subsequent efforts to tame this elusive ligand, albeit with initially limited success, the complex anion *trans*-[Mo(dppe)$_2$(η^1-P≡CSiMe$_3$)(C≡P)]$^-$ being finally inferred by Russell in 2012.[12] More recently, Meyer reported the synthesis of a uranium cyaphide complex (Figure 1), derived from deoxygenation of an $^-$OC≡P ligand,[13] which exhibits a less encumbered coordination sphere, suggesting a greater than anticipated stability for the terminal M–C≡P moiety.

Inspired by Grützmacher's report of **1**,[11] we sought to explore and exploit the potential 'ethynyl-like' character of cyaphide, through its incorporation into complexes of the type *trans*-[Ru(dppe)$_2$(C≡P)(C≡CR)], akin to classical ruthenium bis(acetylide)s. We thus reported in 2014 complexes **3**

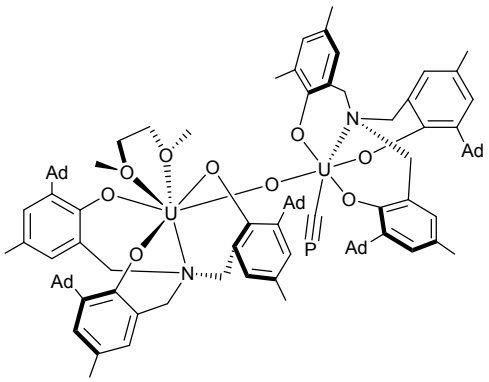

Figure 1: Meyer's uranium-cyaphide complex[13]

[a] Department of Chemistry, University of Sussex, Brighton UK
Email: i.crossley@sussex.ac.uk; Fax: +44 (0)1273 876678; Tel: +44 (0) 1273 877302.

† Footnotes relating to the title and/or authors should appear here.
Electronic Supplementary Information (ESI) available: NMR and UV spectra, computational data, orbital plots, CVs and X-ray diffraction data. CCDC1902212-1902216. See DOI: 10.1039/x0xx00000x

(R = CO_2Me) and **4** (R = C_6H_4OMe-*p*),[14] and more recently the homobimetallic [{(P≡C)(dppe)Ru}$_2${μ-(C≡C)$_2C_6H_4$-*p*)] (**5**),[15] the first compound to incorporate two 'C≡P' moieties within the same conjugate scaffold. In each case, through-conjugation of the acetylenic and cyaphidic π-systems is apparent in both the HOMO and HOMO-1, reminiscent of bis-alkynyl analogues. For **3** and **4** these fragments contribute Intra-Ligand Charge Transfer (ILCT) events ($\pi_{C\equiv C}\rightarrow\pi^*_{C\equiv C}$ and $\pi_{C\equiv P}\rightarrow\pi^*_{C\equiv P}$) to the electronic spectra (*ca* 270 nm),[14] which are otherwise dominated by Metal to Ligand, and Ligand to Ligand Charge Transfers (MLCT/LLCT) from HOMO & HOMO-1 to the low-lying virtual orbitals of the dppe scaffold (LUMO & LUMO+1). The influence of cyaphide upon redox behaviour is also apparent, electrochemical studies of **5**[15] demonstrating a reduced stability of the mixed valence form **5**$^+$ (*cf.* the parent dichloride and analogous alkynyl systems) with concomitant loss of reversibility for both redox events (**5**→**5**$^+$ and **5**$^+$→**5**$^{2+}$).

Following from these preliminary studies, we have sought to develop a deeper understanding of the nature and influence of the cyaphide ligand, and its interaction with *trans*-alkynyl moieties. To this end we describe herein the synthesis of a homologous series of *trans*-cyaphide-alkynyls, and explore the interplay of cyaphide, alkynyl and metal fragments. Aspects of this work have appeared in preliminary form.[14]

Results and discussion

Synthesis

The ruthenium-alkynyl precursors *trans*-[Ru(dppe)$_2$(C≡CR)Cl] (**6**, R = C_6H_4Me-*p* **a**, C_6H_5 **b**, C_6H_4F-*p* **c**, $C_6H_4(CO_2Me)$-*p* **d**, $C_6H_4(NO_2)$-*p* **e**, CO_2Et **f**), are conveniently obtained either directly from literature methods,[14,16] or by their simple modification. Thereafter, halide abstraction in the presence of $Me_3SiC\equiv P$ affords good yields of *trans*-[Ru(dppe)$_2$(η^1-P≡SiMe$_3$)(C≡CR)]$^+$ (Scheme 1, [**7a-f**]$^+$), obtained as either the triflate or hexafluorophosphate salts. In all cases, the identities of **7**$^+$ follow from spectroscopic data, each exhibiting characteristic resonances in the $^{31}P\{^1H\}$ NMR spectrum associated with the η^1-phosphaalkyne (δ_P ~ 110) and dppe (δ_P ~ 40) ligands. Retention of the $SiMe_3$ and alkynyl moieties is in each case apparent from the respective NMR spectroscopic signatures, as is the associated counter-ion (δ_F −78, OTf; δ_F −73.6, δ_P −142.1 (J_{PF} 712 Hz) PF_6). For **7a**$^+$ and **7c**$^+$ single-crystal X-ray diffraction data (*vide infra*) confirmed the structure of the molecular cation.

The conversion of each of **7**$^+$ to the respective cyaphide complexes (**8a-f**) is effected by treatment of thf solutions with stoichiometric KO^{t}Bu. It is noteworthy that this step has proven sensitive to the nature of the counter-ion, **7.OTf** on occasion affording greater purity than the respective **7.PF$_6$**. Moreover, the persistence of any trace silver often results in the contamination of **8** with a phosphacarbon-free complex; while the identity of this species remains elusive, it would appear to result from an oxidative process.[17] This issue is, however, obviated by preparing **7.OTf** from TlOTf (*cf*. AgOTf).

The formation of **8a–f** proceeds rapidly, being complete within 1 hour under ambient conditions, as we have previously described.[14,15] This contrasts starkly Grützmacher's report[11] of a 14-hour reaction time, during which the reversibly-formed [RuH(dppe)$_2${C(SiPh$_3$)=P(OPh)}] (**A**) was observed, resulting from attack of phenoxide base at phosphorus (Scheme 2).[11b] We do not observe any comparable species, even when operating at low temperature (−78 °C) or when using NaOPh in place of KO^{t}Bu; moreover, we have resynthesized **1** using our methodology,[18] thus excluding the influence of the ancillary ligands in respect of this disparity. We thus reason the enhanced susceptibility of the Me_3Si fragment (*cf.* the more encumbered Ph_3Si) toward the attack of base (and thus desilylation) allows this pathway to dominate, precluding formation of a 'dead-end' reservoir species analogous to **A**.

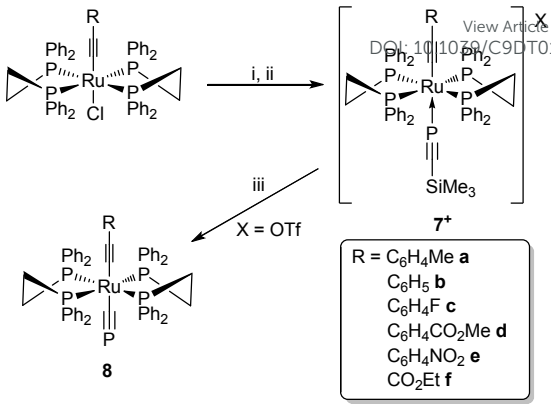

Scheme 1. Synthesis of cyaphide complexes **8a-f**. *Reagents and conditions:* (i) MX (AgOTf, $AgPF_6$, TlOTf), CH_2Cl_2; (ii) P≡CSiMe$_3$, CH_2Cl_2/C_7H_8; (iii) KO^{t}Bu, thf.

The conversions to cyaphide are clearly apparent from spectroscopic changes, which include: i) loss of NMR resonances for the silyl moiety and counter-ion; ii) increased resonant frequency ($\Delta\delta_P$ ~50) for the unsaturated P-centres, with reduced magnitude of the P_{CP}–P_{dppe} coupling; iii) increased frequency ($\Delta\delta_c$ ~90) of the cyaphidic carbon resonance, to a region comparable to that for metal carbonyls and cyanides (δ_C ~ 280); and iv) reduction in frequency of the C≡P stretch ($\Delta\nu_{C\equiv P} \geq -12$ cm^{-1}). Retention of the co-ligands follows from the associated spectroscopic signatures, with the bulk molecular composition confirmed by high-resolution mass spectra. Additionally, both **8c** and **8d** ceded to the growth of single crystals, enabling structural confirmation (*vide infra*).

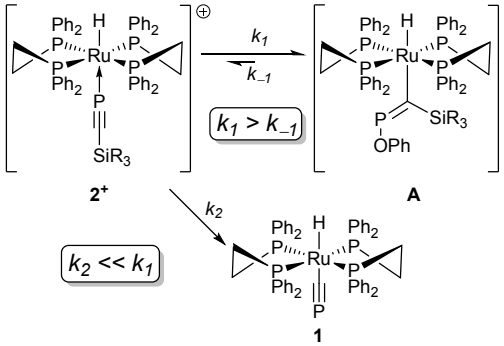

Scheme 2. Reversible formation of a 'dead-end' reservoir species (**A**) upon reaction of **2**$^+$ with NaOPh, intervening in desilylative rearrangement to cyaphide complex **1**.

View Article Online
DOI: 10.1039/C9DT01071H

Table 1: Selected bond distances (Å) and angles (°) for complexes **7a**$^{+}$,[a,b] **7c**$^{+}$,[a,b] **3**, **8c**[c] and **8d**[c] (2 molecules in asymmetric unit) with estimated standard uncertainties in parentheses.

	7a^{+}[a,b]	**7c**$^{+}$[a,b]	**3**	**8c**[c]	**8d**[c,d]	
Ru–P_{PC}	2.264(3)	2.262(1)	-	-	-	-
Ru–C_{CP}	-	-	2.070(6)	2.118(3)	2.076(9)	2.051(11)
Ru–C_{CC}	2.027(9)	2.043(4)	2.053(5)	2.054(20)	2.072(8)	2.072(10)
C≡P	1.515(14)	1.520(5)	1.563(7)	1.493(3)	1.549(10)	1.566(11)
C≡C	1.197(16)	1.182(6)	1.272(9)	1.216(4)	1.216(12)	1.222(13)
C–Si	1.851(14)	1.835(5)	-	-	-	-
Ru–P–C	179.6(6)	179.4(2)	-	-	-	-
Ru–C–P	-	-	169.6(4)	177.8(2)	172.8(6)	172.1(5)
Ru–C–C	175.3(10)	176.2(4)	179.1(5)	178.4(2)	175.1(8)	175.5(7)
P–C–Si	171.8(10)	171.0(4)	-	-	-	-
C–C–C_R	174.4(13)	176.0(5)	169.5(9)	177.6(3)	178.0(10)	176.7(9)
C–Ru–P_{PC}	175.8(3)	175.6(1)	-	-	-	-
C–Ru–C_{CP}	-	-	173.8(2)	174.5(1)	172.4(4)	173.0(3)

[a]PF_6 salt, [b]crystals of the CH_2Cl_2 solvate, [c]Crystals of the benzene solvate, [d]bond distances and angles for **8d** warrant caution, the structure being subject to imperfectly modelled disorder around the dppe backbone. Connectivity can be confidently assigned, with specific geometric parameters subject to significant uncertainty.[19]

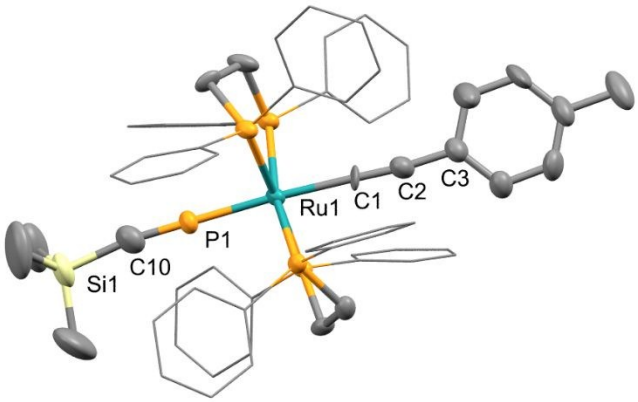

Figure 2. Molecular geometry of **7a**$^{+}$ in crystals of the PF_6 salt as mono CH_2Cl_2 solvate. Solvent, counter ion and hydrogen atoms omitted, and supporting dppe ligands reduced for clarity. Thermal ellipsoids at the 50 % probability level.

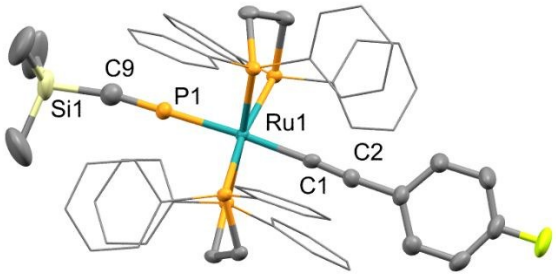

Figure 3. Molecular geometry of **7c**$^{+}$ in crystals of the PF_6 salt as mono CH_2Cl_2 solvate. Solvent, counter ion and hydrogen atoms omitted, and supporting dppe ligands reduced for clarity. Thermal ellipsoids at the 50 % probability level.

Structural Features

The molecular geometries of the phosphalkyne-containing complex cations **7a**$^{+}$ and **7c**$^{+}$, and cyaphide complexes **3**, **8c** and **8d** are illustrated in Figures 2–6 respectively, with selected parameters summarised in Table 1.

Both **7a**$^{+}$ and **7c**$^{+}$ exhibit perfectly linear coordination of the phosphaalkyne moieties, with the trans-alkynyls marginally distorted from linearity. In this respect, both are similar to *trans*-[Ru(dppe)$_2$(η^1-P≡CSiMe$_3$)(C≡CCO$_2$Me)] ($\angle_{RuPC}$ 175.7(4)°; $\angle_{CRuP}$ 177.0(3)°; $\angle_{RuCC}$ 178(1)°),[14] and [{(Me$_3$SiC≡P-η^1)(dppe)Ru}$_2${μ-(C≡C)$_2$C$_6$H$_4$-*p*)] ($\angle_{RuPC}$ 179.3(2)°, 177.3(2)°; $\angle_{CRuP}$ 175.2(2)°, 173.4(2); $\angle_{RuCC}$ 174.2(4)°, 174.5(4)°),[15] which show only marginal deviations, and align well with typical trends for bis-alkynyls[20] and the, still limited, range of complexes featuring an unsupported η^1-phosphaalkyne ligand.[11a,12,21] It is noted that greater deviation from linear coordination was described by Jones for [RuH(dppe)$_2$(η^1-P≡CMe)] ($\angle_{RuPC}$ 153.7(2)°),[22] attributed to interaction (presumably C–H…π) between the phosphaalkyne and flanking phenyl groups, which is obviated by bulkier Me$_3$Si substituents. Accommodation of this bulk does, however, lead to a slight bend within the phosphaalkyne unit, as is noted for most precedent examples, albeit far less pronounced than in **2**$^{+}$ ($\angle_{SiCP}$ 165.5(2)°),[11a] presumably a corollary of the steric footprints of the respective silanes.[23] The remaining internal geometric parameters of **7a**$^{+}$ and **7c**$^{+}$ are similarly consistent with expectation, with P≡C, Ru–P, C≡C and Ru–C≡C linkages all being statistically comparable to relevant precedent examples.

The molecular structures of the cyaphide complexes are somewhat more noteworthy, given the very limited precedent. Both **3** and **8d**[19] exhibit C≡P linkages that are statistically comparable to prior examples (1.573(2) Å **1**; 1.544(4) Å **4**), albeit most closely aligned with **1**. In contrast, that of **8c** appears appreciably shorter, a feature that is accompanied by an extended Ru–C linkage (2.118(3) Å). Though this may be attributed trivially to a reduced $\pi_{Ru}\rightarrow\pi^*_{C\equiv P}$ contribution to ligand binding, there is no evidence for concomitantly enhanced interaction of the *trans*-alkynyl, both Ru–CC and C≡C being statistically comparable to those of **1**, **4** and **8d**.[19] Indeed, solution-phase infrared data for **8c** (ν_{CP} 1245 cm^{-1}; ν_{CC} 2066 cm^{-1}) are in line with the rest of the series and indicate one of the weaker C≡P linkages, features that are also

View Article Online
DOI: 10.1039/C9DT01071H

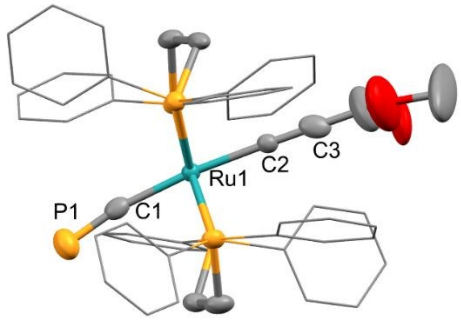

Figure 4. Molecular geometry of **3**, with hydrogen atoms omitted, and dppe ligands reduced for clarity, thermal ellipsoids at the 50 % probability level. The oxygens of the ester group are disordered across multiple sites; omitted for clarity (see ESI).

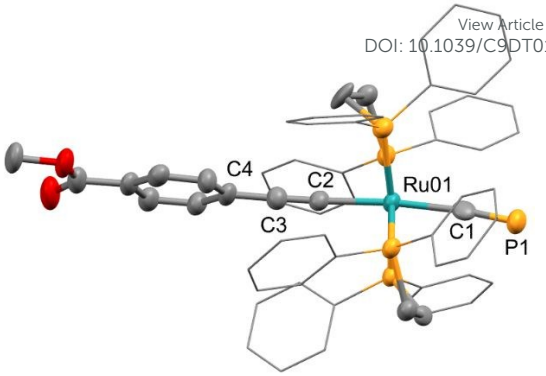

Figure 6. Molecular geometry of **8d** in crystals of the benzene solvate. Hydrogen atoms omitted, and dppe ligands reduced for clarity. The asymmetric unit contains two independent molecules, both of which are illustrated in the electronic supporting information.

mirrored by computational data (see ESI). We thus conclude this to be a crystallographic artefact, warranting caution in discussion of the P≡C moiety within **8c**.

Despite the dearth of structural comparators, there appears to be a general trend toward elongation of the P≡C linkage upon conversion of the η^1-phosphaalkyne ligand into cyaphide, as is also apparent from reduction in ν_{CP}. This would seem consistent with an appreciable $\pi_{Ru}\rightarrow\pi^*_{CP}$ contribution to the bonding of cyaphide, being most pronounced for Grützmacher's **1**, in which competition for back-bonding from ruthenium is obviated by the *trans*-hydride ligand.

The central π-chains of **3**, **8c** and **8d** each exhibit some distortion from linearity, in-line with classical bis(alkynyl) complexes, and indeed **4**. Most pronounced for **3** and **8d**, this is manifest in contraction of ∠Ru–C≡P and ∠C_{CC}–Ru–C_{CP}, which are similar to those in **4** (∠Ru-C-P 172.3(3)°, ∠C-Ru-C 171.9(2)°); in contrast, **8c** shows minimal distortion. Notably, **3** appears to exhibit further deviation at the alkynyl terminus (∠C≡C–C_{ester} 169.5(9)°; C–C_{ester} 1.34(2) Å); while possibly attributable to noted disorder within the ester moiety, DFT studies indicate its retention in the gas-phase, and suggest its origin to lie with partial delocalisation between the ester and alkynyl moieties. Computation data do, indeed, reproduce more generally the structural parameters (see ESI), showing good agreement with experimental data for **8c** and **8d**, and suggesting largely comparable features across the series of complexes. Exception lies with the previously described **4**, for which more linear P–C–Ru, C–Ru–C and Ru–C≡C angles are favoured in the gas phase, as is also apparent for **3**, suggesting a prevalence of packing effects in the solid state.

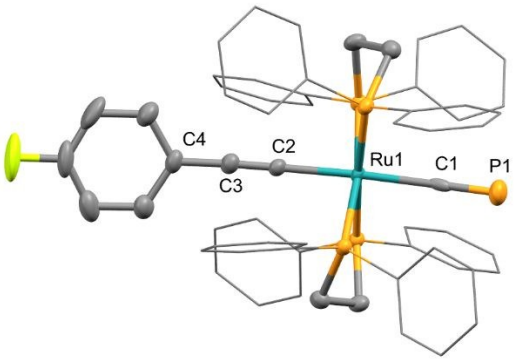

Figure 5. Molecular geometry of **8c** in crystals of the benzene solvate. Hydrogen atoms omitted, and dppe ligands reduced for clarity. Thermal ellipsoids at the 50 % probability level.

Spectroscopic Features

Selected NMR spectroscopic signatures for η^1-phosphaalkyne and cyaphide complexes are summarised in Table 2. For both types of complex, perusal of the data for the *trans*-alkynyl systems reveals general trends in chemical shifts within the phosphacarbon moiety that correlate with the donor/acceptor character of the terminal alkynyl substituent. Thus, for the η^1-P≡$CSiMe_3$ complexes a slight decrease in δ_P is noted in line with increasing electron-withdrawing capacity of the remote substituent, while δ_C exhibits the opposite, far more modest, trend. This is consistent with increasing acceptor character of the "[Ru(dppe)CCR]" fragment inducing polarisation of the phosphaalkynic moiety, manifest as deshielding of the remote carbon centre, with concomitant shielding at phosphorus.

The cyaphidic systems exhibit the reverse trend (increasing

Table 2: Selected NMR spectroscopic data for $[Ru(dppe)_2(C{\equiv}CR)(\eta^1\text{-}P{\equiv}CSiMe_3')]^+$ and [Ru(dppe)(C≡CR)(C≡P)] complexes.

	$Me_3SiC{\equiv}P\rightarrow[Ru]{-}C{\equiv}CR$				[Ru]–C≡P		
R	$\delta_{P(CP)}$[a]	$\delta_{P(dppe)}$[a]	$\delta_{C(CP)}$[a]		$\delta_{P(CP)}$[b]	$\delta_{P(dppe)}$[b]	$\delta_{C(CP)}$[b]
C_6H_4OMe	113.5[c]	42.4[c]	188.2[c]	**4**	159.5[c]	50.8[c]	281.9[c]
7a$^+$	112.3	42.4	188.4	**8a**	159.8	49.8	281.8
7b$^+$	111.9	42.3	188.6	**8b**	160.6	50.9	281.5
7c$^+$	111.9	42.0	188.9	**8c**	161.7	50.8	280.8
7d$^+$	111.0	41.8	190.2	**8d**	165.3	50.7	280.7
7e$^+$	109.1	41.5		**8e**	170.0	50.5	279.5
7f$^+$	108.0[b]	41.3[b]	193.5	**8f**	168.3	44.6	278.7
CO_2Me	108.4[d]	41.2[d]	192.6[d]	**3**	168.5[d]	49.7[d]	279.1[d]
C_6H_4-[Ru]	111.4[e]	42.2[e]	189.8[e]	**5**	159.7[e]	50.7[e]	281.8[e]
[2']$^+$[f]	119.0[d]	60.6[d]	--	**1**	165.0[d]	65.2[d]	287.1[g]

[a]as solutions in $CDCl_3$; [b]as solutions in CD_2Cl_2; [c]as reported in ref 14; [d]redetermined in the present work; [e]as reported in ref 15; [f]$[RuH(dppe)_2(\eta^1\text{-}P{\equiv}CSiMe_3)]^+$; [g]as reported in ref 11 (d_8-THF);

View Article Online
DOI: 10.1039/C9DT01071H

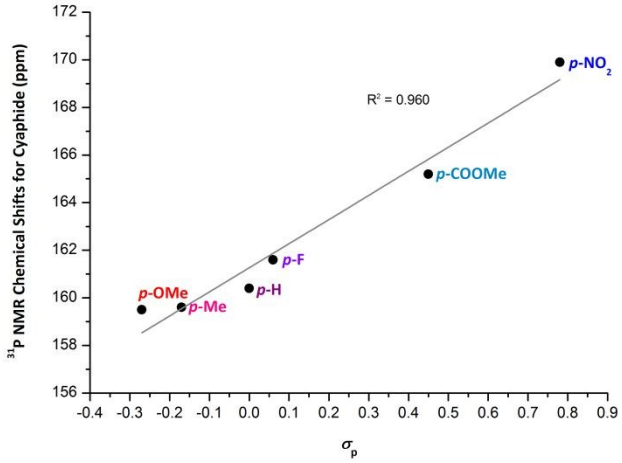

Figure 7: Hammett plot of δ_P vs σ_p for complexes **4** and **8a-e**.

δ_P, decreasing δ_C), which is also appreciably more pronounced values of δ_P in particular spanning over 10 ppm. These effects are clearly illustrated in considering the aromatic alkynyl derivatives (**4** and **8a-e**), Hammett plots (Figures 7 and 8) showing good correlation (R^2 = 0.96) with the σ_p parameter.[24]

Taken together these data suggest a significant long-range influence of the terminal substituent upon the cyaphide moiety, rather than mere modification of acceptor character in the metal-fragment. Indeed, were the latter effect dominant one would anticipate this to be least pronounced for the hydridic **1** (as reflected in data for **2'**$^+$), whereas data for **1** actually lie intermediate to the alkynyl systems. This underlines the interplay between cyaphide and the *trans*-ligand, a long-range communicative regime being consistent with an appreciable level of metal-mediated through-conjugation, as we have previously noted. This defines these complexes as analogues of classical *trans*-bis(acetylide)s, a notion supported by computational data that demonstrate extensive out-of-phase mixing of the Ru (d_{xy}, d_{xz}) C≡C (π) and C≡P (π) in HOMO and HOMO-1 across the series (Figure 9 and ESI), with significant contributions from the cyaphide moiety.

In common with the precedent systems **3 – 5**,[14,15] the low-lying virtual orbitals of **8a-c** are dominated by the Ru(dppe)$_2$

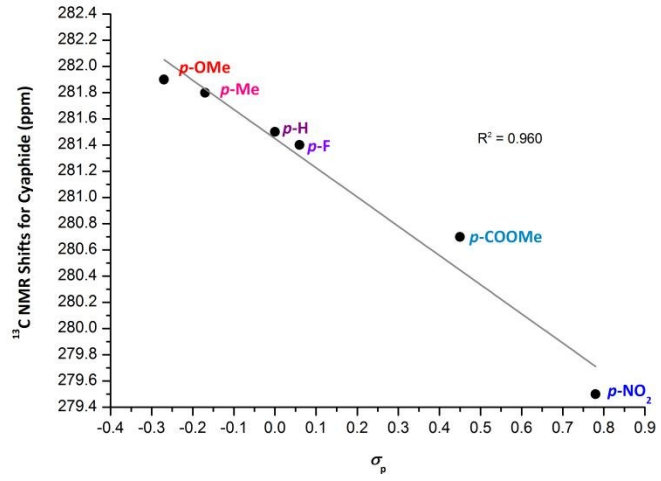

Figure 8: Hammett plot of δ_C vs σ_p for complexes **4** and **8a-e**.

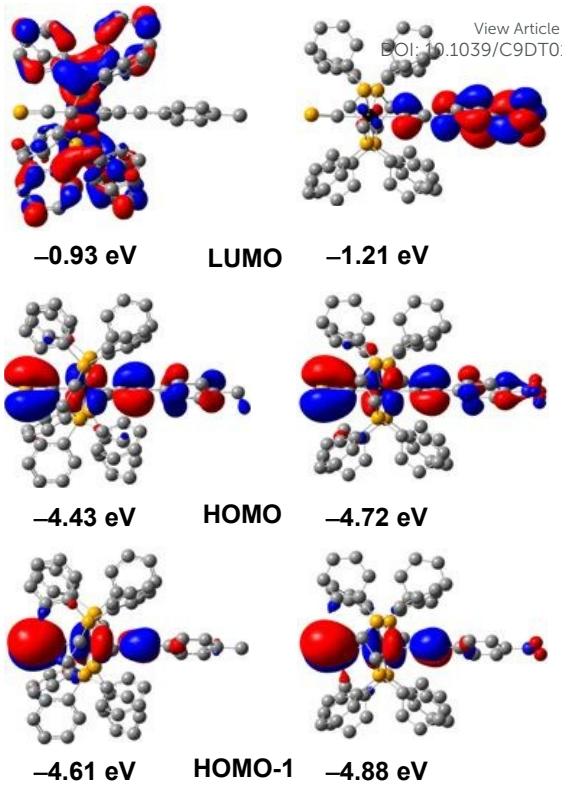

Figure 9. Illustrative frontier orbitals for **8a** (left) and **8e** (right). See ESI for all systems.

scaffold, while the π* orbitals of the C≡P, C≡C and arene moieties contribute significantly only at higher-energy. Thus, the arene fragments feature prominently in orbitals *ca* 4.5 eV above the HOMO (LUMO+11/12 and LUMO+16/17) with modest (*ca* 10%) contributions from the alkynyl π^*_{CC}. The cyaphide π* system contributes heavily (>40%) to LUMO+18/19, *ca* 5 – 5.2 eV above the HOMO. In contrast, the more electron-withdrawing termini of **8d** and **8e** lead to the C_6H_4R moieties dominating LUMO+1 (**8d**) and LUMO (**8e**), which are appreciably stabilised, lying only 3.73 eV and 2.81 eV above the respective HOMOs. Further contributions from the aryl rings are apparent at LUMO+16/19 (**8d**) or LUMO+13/14 (**8e**) at energies comparable to those of **8a-c**. Similarly, π^*_{CP} in each case feature prominently (*ca* 50% or above) around 5 eV above the HOMO (LUMO+17 to LUMO+19).

Unsurprisingly, the electronic spectra of **8a-c** are dominated by LLCT and MLCT transitions from HOMO/HOMO-1 to the supporting dppe ligands (*ca* 300 nm), with similar features noted for both **8d** and **8e**, albeit at slightly lower energy (*ca* 350 nm). Additionally, **8e** exhibits a prominent feature around 460 nm (22000 cm^{-1}) attributable to the HOMO →LUMO excitation and composed of LLCT and MLCT into the nitroarene fragment; higher-energy LLCT/MLCT into the arene fragment are also apparent around 350 nm (28572 cm^{-1}). Similar events associated with MLCT/LLCT into arene-based orbitals are noted across the series around 300 nm (33333 cm $^{-1}$). Additionally, for the less withdrawing termini (**8a-c**) notable contribution from ILCT within both arene and alkynyl fragments is apparent, as is the $\pi_{CP} \rightarrow \pi^*_{CP}$ transition.

View Article Online
DOI: 10.1039/C9DT01071H

TD-DFT studies[25] indicate the latter contributes more prominently to higher energy features from 250 nm (40000 cm^{-1} to 230 nm (43478 cm^{-1}) and is also present within **8d** and 8e, albeit far less prominent. These features are largely reminiscent of our previous observations for **3** and **4** and suggest diminished contribution from ILCT within the cyaphide fragment in line with increasing electron-withdrawing capacity of the remote substituent, presumably a corollary of associated stabilisation of the HOMO/HOMO-1.

Electrochemistry

In order to probe the redox chemistry of the cyaphide complexes, cyclic voltammetry was undertaken for **4** and **8a-e** as CH_2Cl_2 solutions at a platinum disk working electrode (1mm), with NBu_4PF_6 supporting electrolyte. The data are summarised in Table 3 (see also ESI).

In all cases, an irreversible oxidation event is observed, at potentials that become increasingly anodic in line with the electron-withdrawing character of the arene substituent and, broadly, stabilisation of the HOMO. This is illustrated in the Hammett plot (Figure 10) for **4** and **8a-e**, which is broadly consistent with a positive-gradient linear free energy relation, similar to that previously documented for the respective $[Ru(dppe)_2(C{\equiv}CC_6H_4R)Cl]$.[16,26] We note that the correlation is significantly improved on removal of the datum for **8e** (R^2 = 0.94, vs 0.84); indeed, this compound has proven particularly precocious, resisting isolation above 90 % purity and being prone to contamination with electro-active impurities (including the parent **7**.**PF_6**). Our confidence in this datum is thus somewhat limited and warrants caution. Nonetheless, the comparison as a whole does demonstrate a net electron-withdrawing character for the cyaphide moiety, E_{pa} generally lying to more anodic potential than for the respective *trans*-alkynyl chlorides. The situation for **8b** and **8c** is, however, less clear, E_{pa} appearing essentially unchanged from the chloride congeners. In the latter case, this is consistent with a previous report of the complexes $[Ru(dppe)_2X(C{\equiv}CC_6H_4F\text{-}p)]$ (X = Cl, C≡CPh, $C{\equiv}CC_6H_4NO_2$) which also showed near invariance of E_{pa} across the series,[6b] and presumably reflects the synergic $-I/+\pi$ character of the *p*-fluoro substituent, perhaps implying its response to the character of the *trans* ligand. Certainly the present data would seem to suggest some level of cooperativity between the two *trans* disposed ligands across the entire series, further exemplifying their through-conjugate nature. Notwithstanding, the loss of reversibility upon incorporation of cyaphide (*cf.* Cl) suggests destabilisation of the oxidation product, consistent with a net acceptor character for the C≡P moiety. This is consistent with our observation for the homobimetallic **5**,[15] in which this effect was manifest in both reduced stability of the mixed-valence state **5^+** and a marginally more anodic potential for the initial oxidation event.

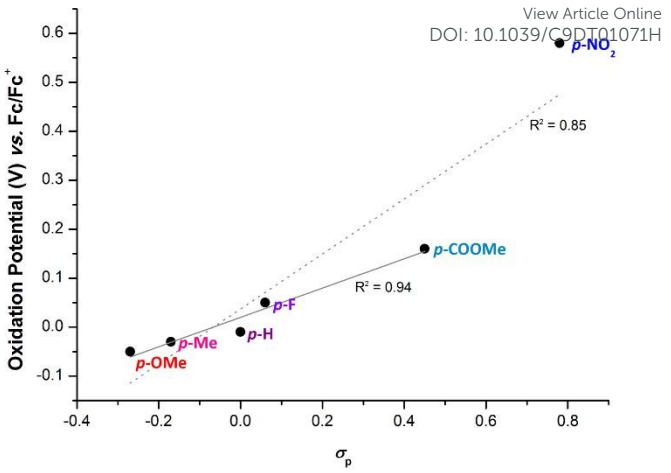

Figure 10. Hammett plot of E_{pa} vs σ_p for **4** and **8a-e**.

The reverse scans reveal a greater variation in behaviour, with **8c** devoid of notable reductive events within the solvent window, while **8e** undergoes a single reduction, close to the solvent break-down potential (*ca* −1.89 V), which is assignable to reduction of the nitro group (*cf.* $[Ru(dppe)_2(C{\equiv}CC_6H_4NO_2)Cl]$, E_{pc} −1.26 V vs SCE;[26] −1.72 V vs Fc/Fc^{+}[27]). In contrast, the remaining systems (**4**, **8a, 8b** and **8d**) each exhibit an irreversible reductive event at appreciably cathodic potential (vs E_{pa}), which are only observable after the initial oxidative sweep, and are thus assigned to the electrogenerated species. In the case of **8d** a second irreversible reduction is observed around −1.70 V, which is similarly attributed, though the lack of consistency across the series precludes any meaningful interpretation in lieu of further data. Unfortunately, efforts to isolate and characterise the oxidation products have thus far proven unsuccessful, chemical oxidation with [Fc]X (X = PF_6, $B(C_6F_5)_4$) thus far yielding no isolable species. *In situ* NMR studies remain inconclusive but would seem to suggest the loss of the cyaphide moiety.

Table 3: Electrochemical (CV) data[a] for **4** and **8a-e**, with comparative data for *trans*-$[Ru(dppe)_2(C{\equiv}CC_6H_4R)Cl]$ ([Ru]–Cl).[b]

	E_{pa} / V[c]	E_{pc} / V[d]	$E_{1/2}$ ([Ru]–Cl)[b]
4	−0.05	−0.90	−0.10[16a]
8a	−0.03	−0.84	−0.03[16a]
8b	−0.01	−0.86	0.01[16a]
8c	0.05	--	0.00[e,25]
8d	0.16	−1.17	0.10[16a]
		−1.70	
8e	0.58	−1.89	0.20[16a]

[a] CH_2Cl_2 / 0.1 M $[NBu_4]PF_6$ using 1 mM analyte solutions at 25 °C with Pt disc (1 mm) working electrode, Pt wire counter electrode and Ag wire pseudo-reference at 100 mV s^{-1}. Potentials relative to the FcH/FcH^+ couple (0.00 V), referenced using internal Fc^*H/Fc^*H^+ (−0.56 V vs FcH/FcH^+). [b] Obtained from cited sources. [c] Irreversible oxidation. [d] Irreversible reduction. [e]re-referenced to Fc/Fc^{+}[26]

Conclusions

We have described the synthesis of a library of homologous cyaphide-alkynyl complexes based around the "$Ru(dppe)_2$" core, demonstrating the breath of both the synthetic protocol and intrinsic stability of the cyaphide ligand within this motif. Spectroscopic data demonstrate a strong and systematic variation in electronic properties upon variation of the

terminal substituent, in line with the σ_p Hammett parameter and indicative of long-range interplay between the terminal sites of the central conjugated scaffold. This aligns with our expectations for the cyaphide-alkynyls to be bis(alkynyl) analogues, as we have previously illustrated, and is supported by DFT data that illustrate comparable distribution of the frontier orbitals to that of their carbocentric congeners. Notwithstanding, the cyaphide-akynyls obtained to date consistently exhibit non-ideal electrochemical behaviour, undergoing irreversible oxidation to give, currently uncharacterised, cyaphide-free species. However, the data do suggest an appreciable linear free energy relation and demonstrate cooperativity between cyaphide and the terminal aromatic substituent. Indeed, comparison with the precedent *trans*-[Ru(dppe)(C≡CC_6H_4R)Cl] demonstrates that replacing Cl^- with "$^-$C≡P" leads generally to more anodic oxidation potentials; however, where R is only marginally electron releasing a negligible effect is apparent. This may hint at a degree of ambivalent behaviour for the cyaphide ligand, making it a potentially valuable addition to the organometallic 'tool-kit', a potential we continue to explore and develop.

Experimental

General methods

All manipulations were performed under anaerobic conditions using standard Schlenk line and glovebox (MBraun) techniques, working under an atmosphere of dry argon or catalytically purified dinitrogen, respectively. Solvents were distilled from appropriate drying agents and stored over either molecular sieves (4 Å; DCM, THF, benzene and Et_2O) or potassium mirrors. General reagents were obtained from Sigma-Aldrich, Fisher or Fluorochem and purified by appropriate methodology prior to use. Compounds **3** and **4**, [Ru(dppe)$_2$Cl]OTf, [Ru(dppe)$_2$(C≡CC_6H_4R)Cl)] (R = OMe, Me, H, CO_2Me, NO_2),[16] $Me_3SiC≡P$[14,28] and NaOPh[29] were prepared using literature methods. NMR spectra were recorded on Varian VNMRS 400 (303 K, ^{1}H 399.50 MHz, ^{13}C 100.46 MHz, ^{19}F 375.87 MHz, ^{31}P 161.71 MHz, ^{29}Si 79.37 MHz), 500 (298 K, ^{1}H 499.91 MHz, ^{13}C 125.72 MHz) or 600 (298 K, ^{1}H 599.69 MHz, ^{13}C 150.81 MHz, ^{31}P 242.83 MHz) spectrometers as indicated. Spectra are referenced to external Me_4Si, 85 % H_3PO_4 and $CFCl_3$ as appropriate. Carbon assignments were made with recourse to the 2D (HSQC, HMBC) spectra, while silicon shifts were obtained indirectly (HMBC). Elemental analyses were obtained either by Mr S. Boyer (London Metropolitan University, Elemental Analysis Service) or Pasher Labs, and were obtained for samples taken from the bulk following final purification. Mass spectra were recorded by Dr A. Abdul-Sada of the departmental service.

We note that a number of systems have defied acquisition of acceptable EA data, despite all other data being indicative of purity.[30] The ESI includes full spectra for all compounds, demonstrating consistent and comparable purity, with HRMS, in lieu of microanalytical data, serving to confirm the identity of the molecular species.

X-ray Diffraction Studies. Single-crystal X-ray diffraction data were recorded on either an Agilent Xcalibur Eos Gemini Ultra or Rigaku XtaLAB AFC11 diffractometer with CCD plate detectors using Cu-K$_\alpha$ (λ = 1.54184 Å) or Mo-K$_\alpha$ (λ = 0.71073 Å) radiation. Structure solution and refinement were performed using SHELXS[31] and SHELXL[31] respectively, running under Olex2.[32]

Crystal Data for 3 (CCDC 1902215). *For* $C_{57}H_{51}O_2P_5Ru.3.5C_6H_6$ (*M* =1359.06 g/mol): triclinic, P-1 (no. 2), *a* = 10.3386(5) Å, *b* = 13.4556(8) Å, *c* = 26.1086(13) Å, α = 82.979(4)°, β = 81.087(4)°, γ = 67.587(5)°, *V* = 3309.1(3) Å^3, *Z* = 2, *T* = 173(2) K, μ(CuKα) = 3.419 mm^{-1}, D_c = 1.302 Mg m^{-3}, 11729 independent reflections, Full matrix F^2 refinement R_1 = 0.0558 on 9839 independent absorption-corrected reflections, [I > 2σ(I); 2θ_{max} = 134.2°], 821 parameters, wR_2 = 0.1495 (all data).

Crystal Data for 7a.PF$_6$ (CCDC 1902212). *For* $C_{65}H_{64}F_6P_6RuSi.CH_2Cl_2$ (*M* =1359.06 g/mol): orthorhombic, $P2_12_12_1$ (no. 19), *a* = 13.5338(4) Å, *b* = 16.2852(4) Å, *c* = 28.7574(8) Å, *V* = 6338.1(3) Å^3, *Z* = 4, *T* = 173(2) K, μ(CuKα) = 4.872 mm^{-1}, D_c = 1.424 Mg m^{-3},), 10598 independent reflections, Full matrix F^2 refinement R_1 = 0.0575 on 8576 independent absorption-corrected reflections, [I > 2σ(I); 2θ_{max} = 142.5°], 743 parameters, wR_2 = 0.1763 (all data).

Crystal Data for 7c.PF$_6$ (CCDC 1902216). For $C_{64}H_{61}F_7P_6RuSi.CH_2Cl_2$ (M = 1363.03 g/mol): orthorhombic, $P2_12_12_1$ (no. 19), a = 13.4662(3) Å, b = 16.1621(4) Å, c = 28.4939(7) Å, *V* = 6201.4(3) Å^3, *Z* = 4, *T* = 173(2) K, μ(MoKα) = 0.570 mm^{-1}, D_c = 1.460 Mg m^{-3}, 13451 independent reflections, full matrix F^2 refinement, R_1 = 0.0344 on 12533 independent absorption corrected reflections [I > 2σ(I); 2θ_{max} = 54.2 °), 742 parameters, wR_2 = 0.0818 (all data).

Crystal Data for 8c (CCDC 1902214). For $C_{61}H_{52}FP_5Ru.2C_6H_6$ (*M* = 1216.16 g/mol): triclinic, P-1 (no. 2), *a* = 11.1652(5) Å, *b* = 15.8226(6) Å, *c* = 17.5577(5) Å, α = 98.356(3)°, β = 93.032(3)°,γ = 104.248(3)°, *V* = 2961.7(2) Å^3, *Z* = 2, *T* = 173(2) K, μ(CuKα) = 3.782 mm^{-1}, D_c = 1.364 Mg m^{-3}, 10532 independent reflections, full matrix F^2 refinement, R_1 = 0.0360 on 8756 independent absorption corrected reflections [I > 2σ(I); 2θ_{max} = 134.0 °), 721 parameters, wR_2 = 0.0817 (all data).

Crystal Data for 8d (CCDC 1902213). For $2\{C_{63}H_{55}O_2P_5Ru\}.2C_6H_6$ (*M* = 2356.19 g/mol): triclinic, P-1 (no. 2), *a* = 9.2841(4) Å, *b* = 24.8606(11) Å, *c* = 26.8008(12) Å, α = 110.850(4)°, β = 90.296(4)°, γ = 93.812(4)°, *V* = 5765.2(5) Å^3, *Z* = 2, *T* = 100(2) K, μ(CuKα) = 3.868 mm^{-1}, D_c = 1.357 Mg m^{-3}, 19809 independent reflections, full matrix F^2 refinement, R_1 = 0.1020 on 12314 independent absorption corrected reflections [I > 2σ(I); 2θ_{max} = 134.2 °), 1365 parameters, wR_2 = 0.3048 (all data).

DFT Calculations. Calculations were performed using Gaussian 09W, Revision C.01,[33] running on an intel i5-2500 (Quad, 3.3 GHz) with 8 GB RAM, or Gaussian 09 Revision D.01,[34] running on the Sussex high Performance Cluster. Results were visualised using Gaussview 5.0; orbital contributions and UV/Vis spectra were obtained using GaussSum.[35] Geometries were optimised with the hybried density functional B3LYP, using the RECP basis set Lanl2dz for

Ru and 6-31G** for all other atoms. Stationary points were characterised using frequency calculations and confirmed as minima on the basis of no imaginary frequencies. Excited states were calculated using TD-DFT with the B3LYP functional, using Lanl2dz for Ru and 3-21G* on other atoms. Influence of a solvent model was assessed but found to not be significant for the present discussion.

Electrochemistry. Cyclic Voltammagrams were obtained under anaerobic conditions, (MBraun glovebox, under catalytically purified dinitrogen) at 298 K, for CH_2Cl_2 solutions (0.1 nM) with 0.1 M $[^nBu_4N]PF_6$ supporting electrolyte, using a three-electrode set-up, comprising platinum disk working electrode (1 mm diameter), platinum wire counter electrode and silver wire pseudoreference. Data were recorded using a PalmSens EmStat3+ Blue potentiostat and the PSTrace software package. Potentials are reported relative to the ferrocene/ferrocinium (FcH/FcH^+) coule, referenced to the FcH^*/FcH^{*+} couple of a doped sample (−0.56 V relative to $FcH.FcH^+$).

Synthesis

[Ru(dppe)$_2$C≡CCO$_2$Et)Cl] (6f). To a stirred solution of $[Ru(dppe)_2Cl]OTf$ (2.00 g, 2.06 mmol) in CH_2Cl_2 was added ethyl propiolate (0.210 cm^3, 2.06 mmol) and the mixture left to stir for 16 h. Removal of the solvent under reduced pressure afforded a brown powder, which was washed with hexanes (3 x 20 cm^3) to yield the intermediary vinylidene salt $[Ru(dppe)_2\{C=C(H)(CO_2Et)\}Cl]OTf$ in adequate purity for further use. $^{31}P\{^1H\}$ ($CDCl_3$): δ 41 (s, 4H). ^1H ($CDCl_3$): δ 7.5 (*t*, *J* = 6.5, 4H), δ 7.4 (*t*, *J* = 7.4, 4H), δ 7.3 (*m (br)*, 8H), δ 7.2 (*m (br)*, 8H), δ 7.1 (*t, J* = 7.6, 8H), δ 3.7 (*q*, *J* = 7.1 Hz ,2H), δ 3.4 (*m (br)*, 1 H), δ 2.9 (*m (br)*, 8H), δ 1.0 (*t*, *J* = 7.1 Hz ,3H). $^{13}C\{^1H\}$-NMR (CD_2Cl_2, 100.5 MHz, 303 K) δ_C: 342.1 (qnt. ($^2J_{CP}$ = 12.68 Hz), Ru=*C*), 163.3 (s, *C*=O), 134.3 (dqnt. (*J* = 78.48, 2.54 Hz), C_6H_5), 131.9 (d (*J* = 57.04), C_6H_5), 130.7 (dqnt. (*J* =84.34, 11.59 Hz), *ipso*-C_6H_5), 129.0 (dqnt. (*J* = 54.88, 2.40 Hz), C_6H_5), 106.1 (s, Ru=C=*C*), 61.2 (s, OCH_2), 29.6 (quint. ($^1J_{CP}$ = 11.33 Hz), C_2H_4), 14.60 (s, CH_3).

The vinylidene salt (2.039 g, 1.91 mmol) was redissolved in CH_2Cl_2 (ca 20 cm^3) followed by the addition of DBU (0,6 cm^3, 4.01 mmol) and the mixture stirred for 3 h at ambient temperature. The solvent was removed under reduced pressure and the residue washed with degassed methanol (3 x 20 cm^3) to yield **6f** as a cream solid. Yield: 1.27 g, 65 %. $^{31}P\{^1H\}$ ($CDCl_3$): δ 48 (s, 4H). ^1H ($CDCl_3$): δ 7.4 (*m*, 8H), δ 7.3 (*m*, 8H), δ 7.2 (*q*, *J* = 7.4, 5.3 Hz , 8H), δ 7.0 (*q*, *J* = 7.17 Hz , 16H), δ 4.0 (*q*, *J* = 7.1 Hz ,2H), δ 2.7 (*m (br)*, 8H), δ 1.2 (*t*, *J* = 7.1 Hz ,3H). $^{13}C\{^1H\}$-NMR ($CDCl_3$, 100.5 MHz, 303 K): δ_C 152.2 (s, C=O), 141.3 (qnt. ($^2J_{CP}$ = 14.70 Hz), Ru–*C*≡C), 135.5 (m, *ipso*-C_6H_5), 134.7 (m (br), C_6H_5), 134.2 (m (br), C_6H_5), 129.1 (d (*J* = 19.09 Hz), C_6H_5), 127.4 (m (br), C_6H_5), 127.2 (m (br), C_6H_5), 107.1 (s, Ru–C≡*C*), 59.3 (s, OCH_2), 30.6 (qnt. ($^1J_{CP}$ = 11.80 Hz), C_2H_4), 15.0 (s, CH_3). ν_{max}/cm^{-1} 2049 (CC). Anal. Found: C, 66.35 %; H, 5.01 %. Calcd for $C_{57}H_{53}P_4O_2ClRu$: C, 66.44 %; H, 5.14 %.

[Ru(dppe)$_2$(C≡CC$_6$H$_4$Me)(η^1-P≡CSiMe$_3$)]$^+$ (7a$^+$). To a stirred solution of [Ru(dppe)(C≡CC$_6$H$_4$Me)Cl] (517 mg, 493 μmol) and $Me_3SiC{\equiv}P$ (0.088 M in toluene, 7 cm^3, 616 μmol) in dichloromethane (ca 20 cm^3) was added *either* $AgPF_6$ (125 mg, 493 μmol) or TlOTf (174 mg, 493 μmol) as suspension in dichloromethane (ca 10 cm^3). The mixture was allowed to stir for 1 h at ambient temperature, the resulting precipitate being removed by filtration (cannula). Removal of the volatiles as reduced pressure afforded a brown solid, which was recrystalized from dichloromethane/pentane to afford the pure salt. Characterized as **7a.PF$_6$**, yield: 540 mg, 86 %. M.p. 179 °C (dec. uncorrected). ^1H NMR: (399.5 MHz, $CDCl_3$) δ_H 7.73 – 7.66 (m, 8H, C_6H_5), 7.38 (m, 4H, C_6H_5), 7.33 (m, 4H, C_6H_5), 7.16 (m, 8H, C_6H_5), 7.11 – 7.01 (m, 18H, C_6H_5 and C_6H_4), 6.74 (d, $^3J_{H-H}$ = 7.9 Hz, 2H, C_6H_4), 2.83 (br m, 8H, PCH_2CH_2P), 2.36 (s, 3H, *p*-CH_3), -0.12 (s, 9H, Si(CH_3)$_3$). $^{31}P\{^1H\}$ NMR (162 MHz, $CDCl_3$): *δ* 112.3 (quint., $^2J_{P-P}$ = 33.3 Hz, 1P, *P*≡C-Si(CH_3)$_3$), 42.3 (d, $^2J_{P-P}$ = 33.3 Hz, 4P, *P*CH_2CH_2P), -144.5 (sept., $^1J_{P-F}$ = 710 Hz, $^-PF_6$). $^{13}C\{^1H\}$ NMR (100 MHz, $CDCl_3$): *δ* 188.4 P≡*C*-Si(CH_3)$_3$, indirect observation), 136.2 (C_6H_4), 134.2 (m, C_6H_5), 132.6 (m, C_6H_5), 130.9 (C_6H_5), 129.9 (C_6H_4), 129.1 (C_6H_4), 128.5 (dt, J_{P-C} = 17.8, 2.5 Hz, C_6H_5), 124.2 (C_6H_5), 116.8 (Ru-C≡*C*-, indirect observation), 30.8 (m, PCH_2CH_2P), 21.5 (*p*-CH_3), 0.31 (br s, Si(CH_3)$_3$). ^{19}F NMR (376 MHz, $CDCl_3$): *δ* -73.8 (d, $^1J_{P-F}$ = 710 Hz, $^-PF_6$). ^{29}Si NMR (79 MHz, $CDCl_3$): *δ* -13.2 (P≡C-*Si*(CH_3)$_3$, indirect observation). IR *ν*/cm^{-1}: 1269 (C≡P), 2112 (C≡C). Elem. Anal. Calc. for $C_{65}H_{64}F_6P_6RuSi$ C: 61.27 %; H: 5.06 %; Found C: 61.07 %; H: 5.00 %.

[Ru(dppe)$_2$(C≡CC$_6$H$_5$)(η^1-P≡CSiMe$_3$)]$^+$ (7b$^+$). In analogous fashion to **7a$^+$**, the crude material was afforded as a yellow oil, which was treated by the addition and evaporation of dichloromethane (5 cm^3) to assist with the azeotropic removal of residual toluene. Pure **7b** was obtained as a yellow solid, characterized as **7b.PF$_6$**, yield 170 mg, 53 %. ^1H NMR (399.5 MHz, C_6D_6): *δ* 7.68 (br m, 8H, *o*-C_6H_5), 7.39 (t, 4H, $^2J_{H-H}$ = 7.3 Hz, *p*-C_6H_5), 7.33 (t, 4H, $^2J_{H-H}$ = 7.3 Hz, *p*-C_6H_5), 7.23 [m, 3H, *m*/*p*-Ph], 7.17 (t, 8H, $^2J_{H-H}$ = 7.3 Hz, *m*-C_6H_5], 7.10-7.02 (m, 16H, *o*/*m*-C_6H_5), 6.82 (d, 2H, $^2J_{H-H}$ = 7.3 Hz, *o*-Ph), 2.86 (m, 8H, $^2J_{H-H}$ = 8.0 Hz, C_2H_4), −0.11 (S, 9H, Si(CH_3)$_3$). $^{31}P\{^1H\}$ NMR (162 MHz, C_6D_6): *δ* 111.9 (quint, $^2J_{P-P}$ = 33.8 Hz, 1P, *P*≡C-Si(CH_3)$_3$), 42.3 (d, $^2J_{P-P}$ = 33.8 Hz, 4P, *P*CH_2CH_2*P*), −144.3 (sept, $^1J_{P-F}$ = 713 Hz, $^-PF_6$). $^{13}C\{^1H\}$ NMR (100 MHz, C_6D_6): *δ* 190.0 (d, $^2J_{C-P}$ = 88 Hz, P≡*C*-Si(CH_3)$_3$), 134.5 (br m, $^2J_{C-P}$ = 10 Hz, *ipso*-C_6H_5), 134.2 (m, *o*-C_6H_5), 132.9 (m, *o*-C_6H_5), 131.0 (s, *p*-C_6H_5), 130.1 (m, *o*-Ph), 128.5 (br m, *m*-C_6H_5), 128.4 (br m, *m*-C_6H_5), 126.3 (s, Ph), 116.2 (s, Ru-C≡*C*), 108.6 (s, Ru-*C*≡C), 30.8 (quint., $^2J_{C-P}$ = 12 Hz, C_2H_4), 0.5 (s, Si(CH_3)$_3$). $^{29}Si\{^1H\}$ NMR (79 MHz, C_6D_6, MHz): *δ* −13.1 (P≡C-*Si*(CH_3)$_3$, indirect observation). IR *ν*/cm^{-1}: 1265 (C≡P), 2091 (C≡C). Anal. Calcd for $C_{64}H_{52}F_6P_6RuSi$: C; 60.98 %, H; 4.96 %. Found: C; 61.09 %, H; 4.97 %

[Ru(dppe)$_2$(C≡CC$_6$H$_4$F)(η^1-P≡CSiMe$_3$)]$^+$ (7c$^+$). In analogous fashion to **7a$^+$**, the crude material was obtained as a pale brown solid, which was washed with benzene, then recrystallized from dichloromethane / pentane. Characterized as **7c.PF$_6$**, yield 412 mg, 65 %. M.p. 208 °C (dec. uncorrected). ^1H NMR: (399 MHz, $CDCl_3$) δ 7.65 – 7.53 (m, 8H, C_6H_5), 7.34 (m, 9H, C_6H_5), 7.14 (m, 8H, C_6H_5), 6.96 (m, 15H, C_6H_5), 6.90 (m, 2H, *o*-C_6H_4), 6.70 (m, 2H, *m*-C_6H_4), 2.84 (br m, 8H, PCH_2CH_2P), -0.13 (br s, P≡C-Si(CH_3)$_3$). $^{31}P\{^1H\}$ NMR: (162 MHz, $CDCl_3$) δ 111.9 (quin, $^2J_{P-P}$ = 33.7 Hz, 1P, *P*≡C-Si(CH_3)$_3$), 42.0 (d, $^2J_{P-P}$ = 33.0 Hz,

4P, PCH_2CH_2P), -142.1 (sept., $^1J_{P-F}$ = 712 Hz, 1P, $^-PF_6$). $^{13}C\{^1H\}$ NMR: (100 MHz, $CDCl_3$) δ 188.9 (P≡*C*-Si$(CH_3)_3$, indirect observation), 161.1 (d, $^1J_{C-F}$ = 247 Hz, *p*-C_6H_4), 133.9 (m, C_6H_5), 133.4 – 131.9 (m, C_6H_5), 131.4 (d, $^3J_{C-P}$ = 8.0 Hz, *o*-C_6H_4), 130.8 (d, $^4J_{C-F}$ = 2.8 Hz, *ipso*-C_6H_4), 128.3 (dt, J_{C-P} = 21.5, 2.3 Hz, C_6H_5), 123.0 (br s, Ru-*C*≡C), 117.8 (s, Ru-C≡*C*-) 115.3 (d, $^2J_{C-F}$ = 21.7 Hz, *m*-C_6H_4), 30.5 (quin., J_{C-P} = 30.4 Hz, P*C*H_2*C*H_2P), 0.28 (br s, P≡C-Si(*C*$H_3)_3$). ^{19}F NMR (376 MHz, $CDCl_3$): -73.6 (d, $^1J_{P-F}$ = 712 Hz, $^-PF_6$), -113.0 (m, *pF*-C_6H_4). ^{29}Si NMR (79 Hz): *δ* -12.9 (P≡C-*Si*$(CH_3)_3$, indirect observation). IR *ν*/cm^{-1}: 1269 (C≡P), 2106 (C≡C). Anal Calcd for $C_{64}H_{61}F_7P_6RuSi$ C: 60.14 %; H: 4.81 %; Found C: 60.75 %; H: 4.61 %

[Ru(dppe)$_2$(C≡C$C_6H_4CO_2Me$)(η^1-P≡C$SiMe_3$)]$^+$ (7d.OTf). In comparable fashion to previous compounds, isolated as a yellow solid. Yield 307 mg, 77 %. M.p. 159 °C (dec. uncorrected). ^1H NMR (399 MHz, $CDCl_3$) δ 7.88 (d, $^1J_{H-H}$ = 8.4 Hz, 2H, *m*-C_6H_4), 7.56 (m, 8H, C_6H_5), 7.39 (m, 4H, C_6H_5), 7.31 (m, 4H, C_6H_5), 7.17 (m, 8H, C_6H_5), 7.04 (m, 16H, C_6H_5), 6.74 (d, $^1J_{H-H}$ = 8.4 Hz, 2H, *m*-C_6H_4), 3.92 (s, 3H), 2.86 (br m, 8H, P*C*H_2*C*H_2P), -0.11 (s, 9H, P≡C-Si(*C*$H_3)_3$)). $^{31}P\{^1H\}$ NMR: (162 MHz, $CDCl_3$) δ 110.9 (m, 1P, *P*≡C-Si$(CH_3)_3$), 41.8 (d, $^2J_{P-P}$ = 33.5 Hz, 4P, PCH_2CH_2P). $^{13}C\{^1H\}$ NMR: (100 MHz, $CDCl_3$) δ 190.2 (P≡*C*-Si$(CH_3)_3$), indirect observation), 167.0 (*C*OOCH_3), 134.2 (m, C_6H_5), 132.9 (m, C_6H_5), 132.4 (m, C_6H_5), 131.1 (m, C_6H_5), 131.0 (d, J_{C-P} = 7.2 Hz, C_6H_5), 129.9 (C_6H_4), 129.7 (C_6H_4), 128.3 (dt, J_{C-P} = 18.5, 2.0 Hz, C_6H_5), 127.5 (C_6H_4), 122.8 (C_6H_4), 119.6 (Ru-*C*≡C-), 115.9 (Ru-C≡*C*-, indirect observation), 52.3 (COO*C*H_3), 30.6 (quin., J_{C-P} = 11.9 Hz, P*C*H_2*C*H_2P), 0.5 (br s, P≡C-Si(*C*$H_3)_3$). ^{19}F NMR (376 MHz, $CDCl_3$): -78.0 (s, -*C*F_3). ^{29}Si NMR (79 Hz, $CDCl_3$): *δ* -12.5 (P≡C-*Si*$(CH_3)_3$, indirect observation). IR *ν*/cm^{-1}: 1265 (C≡P), 1714 (C=O), 2090 (C≡C). MS (HR-ESI$^+$): $[C_{66}H_{65}O_2P_5RuSi]^+$: Calc. 1173.2402; Found 1173.2271.

[Ru(dppe)$_2$(C≡C$C_6H_4NO_2$)(η^1-P≡C$SiMe_3$)]$^+$ (7e$^+$). In analogous fashion to previous examples, the crude material was obtained as a pale brown solid, which was washed with benzene. Characterized as **7e.PF$_6$**, yield 235 mg, 37 %. M.p. 250 °C (dec, uncorrected) ^1H NMR: (399 MHz, $CDCl_3$) δ 8.06 (d, $^3J_{H-H}$ = 8.3 Hz, 2H, C_6H_4), 7.50 (br m, 7H, C_6H_5) 7.40 (m, 5H, C_6H_5), 7.32 (m, 5H, C_6H_5), 7.17 (m, 9H, C_6H_5), 7.06 (m, 14H, C_6H_5), 6.70 (d, $^3J_{H-H}$ = 8.3 Hz, 2H, C_6H_4), 2.87 (br m, 8H, P*C*H_2*C*H_2P), -0.10 (br s, P≡C-Si(*C*$H_3)_3$). $^{31}P\{^1H\}$ NMR: (162 MHz, $CDCl_3$) δ 109.1 (quin, $^2J_{P-P}$ = 34.5 Hz, 1P, *P*≡C-Si$(CH_3)_3$), 41.5 (d, $^2J_{P-P}$ = 33.7 Hz, 4P, PCH_2CH_2P), -144.3 (sept., $^1J_{P-F}$ = 711 Hz, 1P, $^-PF_6$). $^{13}C\{^1H\}$ NMR: (100 MHz, $CDCl_3$) 145.4 (C_6H_4) 133.9 (br, C_6H_5), 132.9 (br, C_6H_5), 132.2 (C_6H_4), 131.2 (d, J_{C-P} = 4.2 Hz), 130.5 (C_6H_4), 128.6 (br d J_{C-P} = 20.7 Hz), 123.9 (C_6H_4), 30.4 (m, P*C*H_2*C*H_2P), 0.23 (br s, P≡C-Si(*C*$H_3)_3$). P≡*C*-Si$(CH_3)_3$ not observed. ^{19}F NMR: (376 Hz, $CDCl_3$): *δ* -73.2 (d, $^1J_{P-F}$ = 715 Hz, $^-PF_6$). ^{29}Si NMR (79 Hz, $CDCl_3$): *δ* -12.5 (P≡C-*Si*$(CH_3)_3$, indirect observation). IR *ν*/cm^{-1}: 1270 (C≡P), 1573 (NO_2), 1314 (NO_2), 2049 (C≡C). Anal. Calcd. for $C_{64}H_{61}F_6NO_2P_6RuSi$ C: 58.90 %; H: 4.71 %; N: 1.07 %; Found C: 58.72 %; H: 4.64 %; N: 1.05 %.

[Ru(dppe)$_2$(C≡CCO_2Et)(η^1-P≡C$SiMe_3$)].OTf (7f.OTf). In similar fashion to the aromatic derivatives, [Ru(dppe)(C≡C$C_6H_4CO_2$Et)Cl] (610 mg, 592 μmol) and TlOTf (219 mg, 619 μmol) were combined as solids, prior to the addition of dichloromethane (ca 20 cm^3). After allowing to stir for 10 min, Me_3SiC≡P (0.0723 M in toluene, 9 cm^3, 651 μmol) was added and the resulting mixture stirred for a further hour. The mixture was filtered and the solvent removed under reduced pressure to afford the crude product, which was washed with benzene (3 x 5 cm^3) and dried *in vacuo*, then recrystalized from dichloromethane. Yield 577 mg, 77 %. ^1H NMR (CD_2Cl_2, 298 K): δ_H 7.45 (12H, *t*, *J* =7.1 Hz, dppe), 7.38 (4H, *t*, *J* = 7.5 Hz, dppe), 7.23 (8H, *t*, *J* = 7.6 Hz, dppe), 7.15 (16H, *t*, *J* = 7.5 Hz, dppe) 4.12 (2H, *q*, *J* = 7.1 Hz, OCH_2), 2.82 (8H, m (br), PC_2H_4P), 1.30 (3H, *t*, *J* = 7.1 Hz, CH_3), -0.1 (9H, *s*, $SiCH_3$). $^{31}P\{^1H\}$ NMR (CD_2Cl_2, 298 K): δ_P 108 (1H, *quint*, *J* = 35 Hz, C≡P$SiMe_3$) 41.3 (4P, *d*, *J = 35 Hz,* dppe). $^{13}C\{^1H\}$-NMR (CD_2Cl_2): δ_C 193.5 (*d, J* = 86 Hz, C≡P) 153.1 (*s*, C=O), 134.1 (*dqnt, J* = 85, 2.4 Hz, C_6H_5), 131.9 (*d, J* = 32 Hz, C_6H_5), 132.5 (*dqnt*, *J* = 214, 11.6 Hz), ipso-C_6H_5), 129.3 (*dqnt, J* = 22, 2.2 Hz, C_6H_5), 123 (*qnt, J* = 321 Hz, Ru–C≡C), 110 (*d (br), J* = 22 Hz, Ru–C≡C), 61.3 (*s*, OCH_2), 30.2 (*qnt, J* = 11.7 Hz, C_2H_4), 15.2 (*s*, CH_3), −0.1 (*s*, $Si(CH_3)_3$). ν/cm^{-1}: 1268 (C≡P), 1688 (CO), 2094 (C≡C). Anal. Calc. for $C_{62}H_{62}F_3O_5P_5SiSRu$: C; 59.09 %, H; 4.96 %. Found: C; 58.85 %, H; 4.92 %.

[Ru(dppe)$_2$(C≡CC_6H_4Me)(C≡P)] (8a). To a mixture of **7a.OTf** (156 mg, 125 μmol) and KO^{t}Bu (14 mg, 125 μmol) was added tetrahydrofuran (20 cm^3); the mixture was then allowed to stir for 1 h at ambient temperature. The volatiles were removed under reduced pressure and the residue extracted into benzene (15 cm^3) and filtered (cannula). The benzene was removed under reduced pressure and the resulting solid washed with hexane, affording **8a** as a yellow solid. Isolated yield 65 mg, 50 %. M.p. 188 °C (dec. uncorrected). ^1H NMR: (399 MHz, CD_2Cl_2) *δ* 7.60 (br m, 6H), 7.51 (br m, 7H), 7.34 - 6.80 (m, 29H), 6.65 (d, J_{H-H} = 7.8 Hz, 2H), 2.88 (br m, 4H, P*C*H_2*C*H_2P), 2.65 (br m, 4H, P*C*H_2*C*H_2P), 2.29 (s, 3H, *p*-CH_3). $^{31}P\{^1H\}$ NMR: (162 MHz, CD_2Cl_2): δ 159.6 (br s, 1P, C≡*P*), 50.8 (d, $^3J_{P-P}$ = 5.2 Hz), 4P, PCH_2CH_2P). $^{13}C\{^1H\}$ NMR: (100 MHz, CD_2Cl_2) δ 281.8 (br, *C*≡P), 137.0 (dquin, J_{C-P} = 172.2 Hz, 11.1 Hz, C_6H_5), 134.9 – 135.4 (br m, C_6H_5), 133.5 (s, C_6H_4), 130.2 (br s, C_6H_5), 129.5 (d, J_{C-P}= 18.4 Hz, C_6H_5), 128.9 (s, C_6H_4) 128.8 (C_6H_4), 127.7 (br m, C_6H_5) 127.5 (dt, J_{C-P} = 22.5, 2.2 Hz, C_6H_5), 119.6 (br, Ru-C≡*C*-), 31.7 (quin, J_{C-P} = 12.0 Hz, P*C*H_2*C*H_2P), 21.5 (*p*-*C*H_3). Ru-*C*≡C- not observed. IR *ν*/cm^{-1}: 1248 (C≡P), 2065 (C≡C). MS (HR-ESI$^+$): $[C_{62}H_{55}P_5Ru]^+$: Calc. 1056.2030; Found 1056.2044; $[M+H]^+$: Calc. 1057.2108; Found 1057.2071.[30]

[Ru(dppe)$_2$(C≡CC_6H_5)(C≡P)] (8b). To a mixture of **7b.PF$_6$** (120 mg, 100 μmol) and KO^{t}Bu (11 mg, 100 μmol) was added tetrahydrofuran (10 cm^3); the mixture was then allowed to stir for 1 h at ambient temperature. The mixture was filtered, and the solvent removed under reduced pressure to afford a pale orange solid. Isolated yield 63 mg, 60 %. ^1H NMR (399 MHz, CD_2Cl_2): *δ* 7.60 (br m, 8H, *o*-C_6H_5), 7.53 (br m, 8H, *o*-C_6H_5), 7.45 (br m, 2H, *m*-Ph), 7.27 (t, 4H, $^1J_{H-H}$ = 7.5 Hz, *p*-C_6H_5), 7.20 (t, 4H, $^1J_{H-H}$ = 7.5 Hz, *p*-C_6H_5], 7.12 (s, 1H, s, *p*-Ph), 7.08 (t, 8H, $^1J_{H-H}$ = 6.9 Hz, *m*-C_6H_5), 6.97 (t, 8H, $^1J_{H-H}$ = 6.9 Hz, *m*-C_6H_5], 6.75 (d, 2H, $^1J_{H-H}$ = 7.5 Hz, *o*-Ph), 2.78 (br dm, 8H, $^1J_{H-P}$ = 94.5 Hz, C_2H_4). $^{31}P\{^1H\}$ NMR (162 MHz, CD_2Cl_2): δ 160.4 (br m, 1P, C≡*P*), 50.8 (br d, $^2J_{P-P}$ = 3.5 Hz, P*C*H_2*C*H_2P). $^{13}C\{^1H\}$ NMR (100 MHz, CD_2Cl_2): *δ* 281.5 (br m, *C*≡P), 137.8 (m, $^1J_{C-P}$ = 10 Hz, *ipso*-C_6H_5), 136.1 (m, $^1J_{C-P}$ = 10 Hz, *ipso*-C_6H_5), 135.4, (m, *o*-C_6H_5), 135.2 (br

m, *ipso*-Ph), 135.0 (m, *o*-C_6H_5), 134.7 (br m, *m*-Ph), 130.4 (br s, *o*-Ph), 129.6 (br s, *p*-C_6H_5), 129.4 (br s, *p*-C_6H_5), 128.1 (br s, *p*-Ph), 127.6 (br m, *m*-C_6H_5), 127.4 (br m, *m*-C_6H_5), 123.9 (s, Ru-C≡*C*), 119.8 (br s, Ru-*C*≡C), 31.7 (quint., $^1J_{C\text{-}P}$ = 12 Hz, C_2H_4). IR *v*/cm^{-1}: 1239 (C≡P), 2067 (C≡C). Anal. Calc. for $C_{61}H_{53}P_5Ru$: C; 70.31 %, H; 5.13 %. Found: C; 70.19 %, H; 5.06 %.

[Ru(dppe)$_2$(C≡CC$_6$H$_4$F)(C≡P)] (8c). In comparable fashion to **8a** Isolated yield 97 mg, 73 %. M.p. 215 °C (dec,uncorrected). ^{1}H NMR: (399 MHz, CD_2Cl_2) δ 7.57 (br m, 14H, C_6H_5), 7.28 (m, 4H, C_6H_5), 7.20 (m, 5H, C_6H_5), 7.10 (m, 8H, C_6H_5), 6.97 (m, 8H, C_6H_5), 6.83 (m, 3H, C_6H_5 and C_6H_4), 6.65 (m, 2H, C_6H_4), 2.77 (br d m, $J_{P\text{-}H}$ = 92.7, 8H, PCH_2CH_2P). ^{31}P NMR: (162 MHz, CD_2Cl_2): δ 161.6 (br s, 1P, C≡*P*), 50.8 (d, $^3J_{P\text{-}P}$ = 3.2 Hz, 4P, *P*CH_2CH_2*P*). ^{13}C{^{1}H} NMR: (100 MHz, CD_2Cl_2) δ 280.7 (m, Ru-*C*≡P), 159.7 (d, $^1J_{C\text{-}F}$ = 242.1 Hz, *p*-C_6H_4), 136.3 (dquin, $J_{C\text{-}P}$ = 157.1, 10.2 Hz, C_6H_5), 134.9 – 134.1 (m, C_6H_5), 131.0 (d, $^3J_{C\text{-}F}$ = 7.7 Hz, *o*-C_6H_4), 128.9 (d, *J* = 23.7 Hz, C_6H_5), 126.9 (dt, *J* = 19.8, 2.2 Hz, C_6H_5), 126.2 (br s, *ipso*-C_6H_4), 117.5 (Ru-C≡*C*-), 114.2 (d, $^2J_{C\text{-}F}$ = 21.3 Hz, *m*-C_6H_4), 31.0 (quin, *J* = 12.0 Hz). ^{19}F NMR (376 MHz, $CDCl_3$): -119.3 (m, *pF*-C_6H_4). IR *v*/cm^{-1}: 1245 (C≡P), 2066 (C≡C). MS (HR-ESI$^+$): [$C_{61}H_{52}FP_5Ru$]$^+$: Calc. 1060.1876; Found 1060.1942; [M+H]$^+$: Calc. 1061.1857; Found 1061.1942.[30]

[Ru(dppe)$_2$(C≡CC$_6$H$_4$CO$_2$Me)(C≡P)] (8d). In comparable fashion to **8a** Isolated yield 55 mg, 70 %. M.p. 215 °C (dec., uncorrected). ^{1}H NMR: (399 MHz, CD_2Cl_2) δ 7.75 (d, $^1J_{H\text{-}H}$ = 8.4 Hz, 2H, C_6H_4), 7.60 (br m, 6H, C_6H_5), 7.46 (br m, 6H, C_6H_5), 7.28 (m, 4H, C_6H_5), 7.19 (m, 7H, C_6H_5), 7.09 (m, 9H, C_6H_5), 6.94 (m, 8H, C_6H_5), 6.65 (d, *J* = 8.4 Hz, 1H), 3.86 (s, 3H, COOCH_3), 3.08 – 2.52 (br m, 8H, PCH_2CH_2P). ^{31}P NMR: (162 MHz, CD_2Cl_2): δ 165.2 (br s, 1P, C≡*P*), 50.8 (d, $^3J_{P\text{-}P}$ = 4.1 Hz, 4P, *P*CH_2CH_2*P*). ^{13}C{^{1}H} NMR: (100 MHz, CD_2Cl_2) δ 167.0 (*C*OOCH$_3$), 136.0 (d of mult, $J_{C\text{-}P}$ = 138.9 Hz, *ipso*-C_6H_5), 134.5 (C_6H_4), 134.4 (d, $J_{C\text{-}P}$ = 64.9 Hz, C_6H_5), 132.7 (C_6H_4), 130.65 (C_6H_4), 129.5 (C_6H_4), 128.9 (d, $J_{C\text{-}P}$ = 27.5 Hz), 128.5 (d, *J* = 52.0 Hz, C_6H_5), 126.9 (d, $J_{C\text{-}P}$ = 23.3 Hz, C_6H_5), 124.3 (Ru-C≡*C*-), 51.5 (COO*C*H$_3$), 30.9 (quin, $J_{C\text{-}P}$ = 12.2 Hz, PCH_2CH_2P), Ru-*C*≡P and Ru-*C*≡C- could not be observed. IR *v*/cm^{-1}: 1242 (C≡P), 1710 (C=O), 2064 (C≡C). MS (HR-ESI$^+$): [$C_{63}H_{55}O_2P_5Ru$]$^+$: Calc. 1100.2025; Found 1100.1960; [M+H]$^+$: Calc. 1101.2006; Found 1101.1971.[30]

[Ru(dppe)$_2$(C≡CC$_6$H$_4$NO$_2$)(C≡P)] (8e). In comparable fashion to **8a**. Following extraction into benzene, the crude material was redissolved in dichloromethane and reprecipitated by addition of hexane. The solid was then isolated by filtration and dried in vacuo to afford **8e** as a deep red solid. Isolated yield 100 mg, 55 %. M.p. 138 °C (dec., uncorrected). ^{1}H NMR: (399 MHz, CD_2Cl_2) δ 7.94 (d, $^2J_{H\text{-}H}$ = 8.9 Hz, 2H, C_6H_4) 7.66 (br m, 7H, C_6H_5), 7.40-7.30 (m, 16H, C_6H_5), 7.19 (m, 9H, C_6H_5), 7.11 (m, 8H, C_6H_5), 6.58 (d, 3H, $^2J_{H\text{-}H}$ = 8.9 Hz, 2H, C_6H_4), 2.78 (br d m, $J_{P\text{-}H}$ = 93.0, 8H, PCH_2CH_2P). ^{31}P{^{1}H} NMR: (162 MHz, CD_2Cl_2): δ 169.97 (br s, 1P, C≡*P*), 50.4 (d, $^3J_{P\text{-}P}$ = 4.8 Hz, 4P, *P*CH_2CH_2*P*). ^{13}C{^{1}H} NMR: (100 MHz, CD_2Cl_2) δ 143.46 (C_6H_4), 135.13 (d of mult, $J_{C\text{-}P}$ = 122.9 Hz, *ipso*-C_6H_5), 134.99 (d of mult, $J_{C\text{-}P}$ = 82.1 Hz, C_6H_5), 132.30 (C_6H_4), 131.14 (mult., C_6H_5), 130.41 (C_6H_4), 129.57 (d, $J_{C\text{-}P}$ = 32.8 Hz), 129.18 (m, C_6H_5), 128.72 (C_6H_4), 127.39 (d of mult, $J_{C\text{-}P}$ = 22.5 Hz, C_6H_5), 123.62 (C_6H_4) 120.92 (Ru-C≡*C*-), (quin, $J_{C\text{-}P}$ = 11.4 Hz, PCH_2CH_2P), Ru-*C*≡P and Ru-*C*≡C- could not be observed. IR *v*/cm^{-1}: 1257 (C≡P), 1323 (NO_2), 1579 (NO_2), 2044 (C≡C).[30]

[Ru(dppe)$_2$(C≡CCO$_2$Et)(C≡P)] (8f). In a similar manner to the aromatic derivatives, **7f.OTf** (450 mg, 360 μmol) and KO^{t}Bu (49 mg, 440 μmol) were combined as solids before the addition of tetrahydrofuran (20 cm^3). The resulting orange solution was allowed to stir for 1 h, after which the solvent was removed under reduced pressure until precipitation of KOTf was noted, whereupon the mixture was filtered and the remaining solvent removed under reduced pressure. The resulting solid was washed with degassed water (3 x 10 cm^3), then treated with benzene (10 cm^3) to assist with azeotropic drying at reduced pressure. Pure **8f** was dried in vacuo. Yield 251 mg, 60 %. ^{1}H NMR (CD_2Cl_2, 298 K): δ_H 7.60 (8H, *m (br),* dppe), 7.40 (8H, *m (br),* dppe), 7.29 (4H, *t*, *J* = 7.38 Hz, dppe), 7.21 (4H, *t*, *J* = 7.37 Hz, dppe), 7.10 (8H, *t*, *J* = 7.55 Hz, dppe), 7.0 (8H, *t*, *J* = 7.58 Hz, dppe) 3.97 (2H, *q, J* = 7.1 Hz, OCH_2), 2.7 (8H, m (br), PC_2H_4P), 1.20 (3H, *t, J* = 7.10 Hz, CH_3). ^{31}P{^{1}H} (CD_2Cl_2) NMR: δ_P 168.3 (1H, *m (br)*, P≡C), 44.56 (4H, *d*, *J* = 4.7 Hz, PPh_3). ^{13}C{^{1}H}-NMR (CD_2Cl_2): δ_C 278.7 (*m (br),* C≡P), 152.0 (*s*, C=O), 141.8 (*m (br),* Ru–C≡C), 135.7 (*dqnt, J* = 111, 11 Hz, C_6H_5), 134.9 (*m (br),* C_6H_5), 134.2 (*qnt*, *J* = 2.3 Hz, C_6H_5), 129.0 (*d, J = 40 Hz,* C_6H_5), 127.0 (*dqnt*, *J* = 27.25, 2.12 Hz, C_6H_5), 112.1 (*s*, Ru–C≡C), 59.2 (*s*, OCH_2), 30.8 (*qnt, J* = 11.85 Hz, C_2H_4), 14.6 (*s*, CH_3). ν_{max}/cm^{-1}: 1238 (C≡P), 1647 (CO), 2063 (C≡C). Anal. Calcd. for $C_{58}H_{53}O_2P_5Ru$: C, 67.11 %; H, 5.15 %, Found: C, 66.96 %; H, 5.28 %.

Conflicts of interest

There are no conflicts to declare.

Acknowledgements

We thank the Royal Society, Leverhulme Trust (F/00 230/AL; studentship to N.Trathen), Engineering and Physical Sciences Research Council (EP/N016785/1 and EP/N509784 [DTP studentship 1805157, M.C.Levis]) and the University of Sussex (studentship to M.C.Leech) for financial support. IRC gratefully acknowledges the award of a Royal Society University Research Fellowship. We thank Dr N. Tsoureas and Dr S. M. Roe for assistance with refinement of the crystal data for **3**.

Notes and references

1 For reviews of phosphacarbon and phosphaalkene chemistry see: (a) F. Mathey, *Angew. Chem. Int. Ed.* 2003, **42**, 1578-1604. (b) R. Appel, in *M.* Regitz, O. J. Scherer, *Multiple Bonds and Low Coordination in Phosphorus Chemistry*, Thieme, Stutgart, 1990. (c) L. N. Markovski,; V. D. Romanenko, *Tetrahedron* 1989, **45**, 6019-6090. (d) R. Appel, F. Knoll, I. Ruppert, *Angew. Chem. Int. Ed. Engl.* 1981, **20**, 731-744.

2 K. B. Dillon, F. Mathey, J. F. Nixon, *Phosphorus: The Carbon Copy*, Wiley, Chichester, 1998.

3 See for example: (a) L.-l. Shen, Y. Ye, Y. Lou, L-z. Liu, *Phosphorus, Sulfur and Silicon,* 2010, 680 – 687. (b) C. Jones, C. Schulten, A. Stasch, *Inorg. Chem.*, 2008, **47**, 1273 – 1278. (c) S. Ito, H. Miyake, M. Yoshifuji, *Eur. J. Inorg. Chem.*, 2007,

3491 – 3496. (d) M. A. Hofmann, U. Bergsträßer, G. J. Reiß, L. Nyulászi, M. Rgitz, *Angew. Chem. Int. Engl.* 2000, **39**, 1261 – 1263. (e) F. G. N. Cloke, P. B. Hitchcock, J. F. Nixon, D J. Wilson, P. Mountford, *Chem. Commun.,* 1999, 661 – 662. (f) Rösch, T. Facklam, M. Regitz, *Tetrahedron,* 1987, 43, 3247 – 3256. (g) W. Rösch, M. Regitz, *Angew. Chem. Int. Ed. Engl.*, 1984, 23, 900 – 901.

4 See for example: (a) M. Trincado, A. J. Frosenthal, M. Vogt, H. Grützmacher, *Eur. J. Inorg. Chem.*, 2013, 1599 – 2604. (b) P. L. Arnold, F. G. N. Cloke, J. F. Nixon, *Chem. Commun.*, 1998, 797 – 798. (c) F. Tabellion, A. Nachbauer, S. Leininger, C. Peters, M. Regitz, *Angew. Chem. Int. Ed.*, 1998, **37**, 1233 – 1235. (d) P. L. Arnold, F. G. N. Cloke, P. B. Hitchcock, J. F. Nixon, *J. Am. Chem. Soc.*, 1996, **118**, 7630 – 7631.

5 (a) J. F. Nixon, *Coord. Chem. Rev.* 1995, **145**, 201-258. (b) J. F. Nixon, *Chem. Rev.* 1988, **88**, 1327-1362.

6 V. K. Greenacre, I. R. Crossley, *Inorganics* 2000, ***4***, 30l 1-11

7 J. M. Goicoechea, H. Grützmacher, *Angew. Chem. Int. Ed.*, 2018, **57**, 2 – 31 and references therein.

8 Comp anion

9 H. Jun, V. G. Young Jr., R. J. Angelici, *J. Am. Chem. Soc.*, 1992, **114**, 10064 - 10065.

10 (a) H. Jun, R. J. Angelici, *Organometallics*, 1994, **13**, 2454 - 2460*;* (b) W. V. Konze, V. G. Young, Jr., R. J. Angelici, *Organometallics*, **18**, 258 - 267.

11 (a) J. G. Cordaro, D. Stein, H. Ruegger, H. Grutzmacher, *Angew. Chem. Int. Ed.* 2006, **45**, 6159-6162. (b) T. Groer, G. Baum, M. Scheer, *Organometallics* 1998, **17**, 5916-5919.

12 S. M. Mansell, M. Green, C. A. Russell, *Dalton Trans.* 2012, **41**, 14360-14368.

13 C. J. Hoerger, F. W. Heinemann, E. Louyriac, L. Maron, H. Grützmacher, K. Meyer, *Organometallics,* 2017, **36**, 4351-4354.

14 N. Trathen M. C. Leech, I. R. Crossley, V. K. Greenacre, S. M. Roe, *Dalton Trans.* 2014, **43**, 9004–9007.

15 M. C. Leech, I. R. Crossley, *Dalton Trans.*, 2018, **47**, 4428–4432.

16 (a) M. A. Fox, J. E. Harris, S. Heider, V. Pérez-Gregorio, M. E. Zakrzewska, J. D. Farmer, D. S. Yufit, J. A. K. Howard, P. J. Low, *J. Organomet. Chem.*, 2009, **694**, 2350-2358. (b) J. P. L. Morrall, M. P. cifuentes, M. G. Humphrey, R. Kellens, E. Robijns, I. Asselberghs, K. Clays, A. Persoons, M. Samoc, A. C. Willis, *Inorg. Chim. Acta*, 2006, **359**, 998-1005. (c) S. Margqués-González, M. Parthey, D. S. Yufit, J. A. K. Howard, M. Kaupp, P. J. Low, *Organometallics*, 2014, **33**, 4947-4963.

17 Some evidence for this was obtained by treating both $\mathbf{7}^{+}$ and the parent alkynyl chlorides with $[Fc]PF_6$, resulting in observation of a comparable species, albeit still uncharacterised.

18 M. C. Leech, PhD Thesis, University of Sussex 2018

19 The structure obtained for **8d** constitutes the best refinement achievable with the best data set available, after running several crystals. The structure is subject to significant disorder about the dppe backbone which has defied modelling, and apparent ghosting around ruthenium, the origin of which is unclear. Consequently, while connectivity can be reliably established, caution is required in respect of geometric parameters. Notwithstanding, in respect of the cyaphide fragment these data are consistent with the limited current range of comparators.

20 (a) M. C. B. Colber, J. Lewis, N. J. Long, P. R. Raithby, A. J. P. White, D. J. Williams, *Dalton Trans.*, 1997, 99-104. (b) N. D. Jones, M. O. Wolf, *Organometallics*, 1997, **16**, 1352-1354. (c). C.-Y. Wong, C.-M. Che, M. C. W. Chan, J. Han, K.-H. Leung, D. L. Phillips, K.-Y. Wong, N. Zhu, *J. Am. Chem. Soc.* 2005, **127**, 13997-14007. (d) A. Vacher, F. Barriere, T. Roisnel, L. Piekara-Sady, D. Lorcy, *Organometallics*, 2011, **30**, 3570-3578.

21 (a) T. Groer, G. Baum, M. Scheeer, *Organometallics*, 1998, **17**, 5916-5919. (b) M. F. Medine, M. A. D. D. A. Lemos, A. J. L Pombeiro, J. F. Nixon, P. B. Hitchcock, *J. Chem. Soc., Dalton Trans.*, 1998, 3319 - 3324. (c) P. B. Hitchcock, M. J. Maah, J. F. Nixon, G. J. Leigh, M. A. Bakar, *Angew. Chem., Int. Ed Engl.*, 1987, **26**, 474 - 475. (d) J. G. Cordaro, D. Stein, H. Grützmacher, *J. Am. Chem. Soc.*, 2006, **128**, 14962–14971.

22 C. Jones, C. Schulten, A. Stasch, *Eur. J. Inorg. Chem.*, 2008, 1555–1558.

23 Steric effects were cited as the origin of this 'bend' within $\mathbf{2}^{+}$,[11a] based upon similar observations within other silylalkynyl systems, e.g. (a) K. Vendkatesan, T. Fox, H. W. Schmalle, H. Berke, *Organometallics*, 2005, **24**, 2834–2847. (b) B. siggelkow, M. B. Meder, C. H. Galka, L. H. Gade, *Eur. J. Inorg. Chem.*, 2004, 3424–3435.

24 C. Hansch, A. Leo, R. W. Taft, *Chem. Rev.*, 1991, **91**, 165 – 195.

25 TD-DFT were performed using the B3LYP functional with the 3-21G* basis set across all atoms without addition of a solvent model. Though a relatively low level of theory (a balance against system complexity of required number of excited states) we have conducted comparison studies with a solvent model, and indeed at higher theory across a smaller set of excitation, finding comparable results with only small deviations. We thus consider – as we have previously noted – this level to be adequate to guide assignment of the key features.

26 N. Gauthier, N. Tchouar, F. Justaud, G. Argouarch, M. P. Cifuentes, L. Toupet, D. Touchard, J-F. Halet, S. Righaut, M. G. Humphrey, K. Costuas, F. Paul, *Organometallics* 2009, **28**, 2253-2266.

27 Conversion for CH_2Cl_2 solutions with $[NBu_4]PF_6$ supporting electrolyte, as detailed in: N. G. Connelly, W. E. Geiger, *Chem. Rev.*, 1996, **96**, 877-910.

28 (a) V. K. Greenacre, I J. Day, I .R Crossley, *Organometallics*, 2017, **36**, 435 – 442. (b) V. K. Greenacre, N. Trathen, I. R. Crossley, *Organometallics*, 2015, **34**, 2533 – 2542. (c) N. Trathen, V. K. Greenacre, I. R. Crossley, S. M. Roe, *Organometallics*, 2013, **32**, 2501 – 2504. (d) C. E. Averre, M. P. Coles, I. R. Crossley, I. J. Day, *Dalton Trans*, 2011, **41**, 278 – 284.

29 M. Kunert, E. Dinjus, M. Nauck, J. Sieler, *Chem. Ber.*, 1997, **130**, 1461 – 1465.

30 Spectra (ESI) confirm the absence of NMR active impurities, including residual triflate or PF_6 salts, ^{19}F NMR returning blank spectra (not included). Additionally, MS shows no evidence for metal-based contaminants (e.g. Ag, K, Tl). Analyses are routinely high for carbon, for which we cannot account, including for samples of the pure crystals used in X-ray analysis.

31 G. M. Sheldrick, *Acta Crystallogr., Sect. A: Found. Crystallogr.*, 2008, **64**, 112 – 122.

32 O. V. Dolomanov, L. J. Bourhis, R. J. Gildea, J. A. K. Howard, H. Puschmann, *J. Appl. Crystallogr.*, 2009, **42**, 339 – 341.

33 Gaussian 09, Revision C.01, M.J. Frisch, G.W. Trucks, H.B. Schlegel, G.E. Scuseria, M.A. Robb, J.R. Cheeseman, G. Scalmani, V. Barone, B. Mennucci, G.A. Petersson, H. Nakatsuji, M. Caricato, X. Li, H.P. Hratchian, A.F. Izmaylov, J. Bloino, G. Zheng, J.L. Sonnenberg, M. Hada, M. Ehara, K. Toyota, R. Fukuda, J. Hasegawa, M. Ishida, T. Nakajima, Y. Honda, O. Kitao, H. Nakai, T. Vreven, J.A. Montgomery Jr., J.E. Peralta, F. Ogliaro, M. Bearpark, J.J. Heyd, E. Brothers, K.N. Kudin, V.N. Staroverov, T. Keith, R. Kobayashi, J. Normand, K. Raghavachari, A. Rendell, J.C. Burant, S.S. Iyengar, J. Tomasi, M. Cossi, N. Rega, J.M. Millam, M. Klene, J.E. Knox, J.B. Cross, V. Bakken, C. Adamo, J. Jaramillo, R. Gomperts, R.E. Stratmann, O. Yazyev, A.J. Austin, R. Cammi, C. Pomelli, J.W. Ochterski, R.L. Martin, K. Morokuma, V.G.

View Article Online
DOI: 10.1039/C9DT01071H

Zakrzewski,; G.A. Voth, P. Salvador, J.J. Dannenberg, S. Dapprich, A.D. Daniels, O. Farkas, J.B. Foresman, J.V. Ortiz, J. Cioslowski and D.J. Fox, Gaussian, Inc., Wallingford CT, 2010.

34 Gaussian 09, Revision D.01, authors as above, Gaussian, Inc., Wallingford CT, 2013.

35 N. M. O'Boyle, A. L. Tenderhold, K. M. Langner, *J. Comp. Chem.*, 2008, **29**, 839 – 845.

36 Compound **8e** has proven difficult to obtain in purity, rarely exceeding 90 % and often contaminated by the persistence of **7e.OTf**. Though impure, the data available are appropriate to the discussion and do not compromise the conclusions.

View Article Online
DOI: 10.1039/C9DT01071H

For table of contents use only

A homologous series of cyaphide-alkynyl complexes is prepared and their structural, spectroscopic and electrochemical features probed, revealing significant cooperativity between the -C≡P and remote substituents on the *trans*-alkynyl ligand, indicative of long-range communication; analogy to classical alkynyls is apparent, with cyaphide exhibiting appreciable acceptor character, moderated by the remote substituent.